Article

Single Scattering Albedo's Spectral Dependence Effect on UV Irradiance

Raptis Ioannis-Panagiotis[1,2*], Kazadzis Stelios[2,1], Eleftheratos Kostas [3,4], Amiridis Vassilis[5], Fountoulakis Ilias[6,7]

[1] Institute for Environmental Research and Sustainable Development, National Observatory of Athens, Athens, Greece
[2] Physicalisch-Meteorologisches Observatorium Davos, World Radiation Center, Davos, Switzerland
[3] Department of Geology and Geoenvironment, National and Kapodistrian University of Athens, Greece
[4] Centre for Environmental Effects on Health, Biomedical Research Foundation of the Academy of Athens, Athens, Greece
[5] Institute for Astronomy, Astrophysics, Space Applications and Remote Sensing, National Observatory of Athens, Athens, Greece
[6] Aosta Valley Regional Environmental Protection Agency (ARPA), Saint-Christophe, Italy
[7] Laboratory of Atmospheric Physics, Aristotle University of Thessaloniki, Thessaloniki, Greece

* Correspondence: piraptis@meteo.noa.gr

Abstract The Absorbing/scattering nature of aerosols affects the total radiative forcing and this absorption to total extinction ratio is quantified by single scattering albedo (SSA). Effect of SSA in the Ultraviolet (UV) irradiance is less studied and limited measurements are available. SSA retrieved at Athens, Greece during 2009-2014 from Ultraviolet Multifilter Radiometer (UVMFR) at 332 and 368 nm, were used to calculate incoming UV irradiance, alongside with ones from AERONET at visible wavelengths, from OMI satellite at 342.5 nm and from AEROCOM climatological database at 300 nm. UVA and UVB irradiances were estimated using a Radiative Transfer Model and we found that relative differences could be as high as 20%, while average relative differences varied from 2% to 8.7 % for the whole experimental period. Both UVA and UVB drop by a rate of ~12% for 0.05 aerosol absorption optical depth compared to ones estimated using SSA at visible range. Brewer irradiance measurements at 324nm were used to validate simulated irradiances and a better agreement was found when UVMFR SSAs were used with an average difference of 0.86%, while when using visible or climatological input, relative differences were estimated +4.91 and +4.15% accordingly.

Keywords: Solar Irradiance; SSA; Ultraviolet; Aerosols; Radiative Transfer; Absorption; UVA; UVB;

1. Introduction

Aerosols are among the major agents of Earth's radiative budget, having a crucial effect on the climate. Aerosols directly absorb solar irradiance and contribute to the heating of the Atmosphere. Furthermore, they reduce the planetary albedo, either directly or by enhancing the absorption of solar and terrestrial radiation by

clouds [1]. Thus, their presence affects the thermal state of the atmosphere having both a heating and a cooling effect. The highest uncertainties of anthropogenic climate change are caused by factors controlling aerosol forcing. A recent comprehensive review of the current state of knowledge on aerosol effect on radiation and climate is provided by IPCC [2], estimated the total direct forcing of aerosols in the scale of -0.45 W/m2, though with uncertainty more than 100%. One of the major sources of uncertainty in contemporary modelled aerosol climate forcing is the absorbing/scattering nature of the particles. Spectral dependence of columnar absorbing characteristics of aerosols causes changes in the radiative forcing of the atmosphere and the climate. Columnar aerosol absorption of Ultraviolet (UV) Irradiance is even less studied but has significant effect as it strongly influences photolysis rates and indirectly affects agricultural productions and human health [3,4].

The aerosols that show a significant absorbing behaviour are mainly black carbon, mineral dust and organic aerosols grouped as brown carbon [3]. Absorption of urban aerosols is more efficient in the UV than in visible wavelengths [5]. Jethva and Torres [6] found evidence that absorption from biomass burning aerosols has a significant spectral dependence, showing significant effects at the UV part of the solar spectrum. Corr et al. [7] presented a significant enhancement of columnar aerosol absorption in the UV region, in Mexico City, which was attributed to increased organic carbon components in the aerosol mixture. More recent studies [3,8] attributed the large differences between visible and UV columnar absorption to brown carbon emitted from biomass burning.

The most commonly used variable for monitoring aerosols in the atmosphere is the aerosol optical depth (AOD) which is retrieved by ground-based [9,10] and satellite instruments [11]. One important variable for the radiative transfer calculations is Single Scattering Albedo (SSA), which is defined as the ratio of scattering to total extinction. Thus, it is linked to the chemical composition and the size of the particles. High SSA signifies more scattering aerosols, while lower values are linked to more absorbing types. SSA value determines the cooling/warming outcome of the aerosol radiative forcing effect [12]. Thus, uncertainties in the estimation of SSA lead to changes on the sign of forcing. Also, SSA is strongly spectral depended, demonstrating different behaviour according to aerosol mixture which may lead to significant changes as a function of wavelength [13]. SSA used in radiative transfer model (RTM) calculations refers to the vertical profile (column) of the aerosol extinction coefficient that usually differs significantly from the in-situ measured one [8]. These profiles of the extinction coefficient can be retrieved by airborne in situ vertical profiling of aerosols [14,15,16] but this approach remains very expensive and is rarely used, in experimental campaigns. More commonly, retrievals of the mean columnar SSA from sun-photometric instruments are used to scale default climatological profiles used for RTM simulations. Measurements of the mean columnar SSA are available from a large number of sites around the globe, though rarely in the UV [8,17].

Regarding the Visible and near Infrared spectral range, there are datasets available for SSA retrievals from the most common sun-photometric networks. The Aerosol Robotic Network (AERONET) provides SSA in that range using an inversion algorithm [18]. The international network for aerosol, clouds and solar radiation studies and their applications (SKYNET) [19,20] also retrieves SSA at visible wavelengths while recently efforts were made to also provide SSA at 340 and 380nm [17]. Still, datasets of SSA in the UV spectral region retrieved from ground-based measurements are not frequent and usually are available for short periods of time, while in the scientific literature there are a few publications on the subject [4, 7, 8, 17, 21-24]. UVMFR measurements are used in some of the above studies to retrieve SSA in UV wavelengths following the methodology described in Kroktov et al. [22,23].

SSA in the UV spectral region is also retrieved from satellite sensors. Ozone Monitoring Instrument (OMI) boarded on AURA (NASA's satellite) measures reflected radiation from the Earth's surface at 270-500 nm spectral range. OMAERUV algorithm [25,26] is used to retrieve AOD and SSA at 20 wavelength bands. SSA in UV is retrieved for the bands with central wavelengths at 388nm and 342.5nm. SSA retrieved from this algorithm has been assessed, compared to AERONET retrievals at visible wavelengths [6, 25, 27, 28], though both inversion techniques use several assumptions and, thus, are not directly comparable. Jethva et al. [28] found that the highest differences of satellite and ground-based SSA are over the Arabian Peninsula, biomass burning areas in Southeast Asia and Australia, and occasionally, above urban sites around the globe.

UV irradiance is less than 10% of the solar irradiance reaching the Earth surface, but it is very important for the biosphere. UV solar spectrum is divided in three zones: UVC (<290nm), where practically all irradiance is blocked by the atmosphere; UVA (315-400 nm), which provides ~90% of the total UV radiation reaching the surface; and UVB (290-315 nm), which is the most harmful for living cells and at the same time beneficial for humans since it alters the creation of vitamin D in the human skin [29,30]. Ozone is the dominant attenuator of UVB irradiance and the most important atmospheric factor for its deviations (31). Aerosol attenuation in UV spectral region is also a non- negligible factor for the irradiance reaching the surface and, in some cases, its effects have been found to be as important as those of ozone [32-35]. Also, aerosols affect indirectly the variability of UV radiation, since tropospheric ozone concentration may widely vary due to changes in absorbing aerosols that alter UV and thus the photochemistry of the lower atmosphere [35].

Several factors related to human health are actively related to UV Irradiance estimation, such as DNA damage, Vitamin D Effective Dose and the UV index (erythema) for human exposure to the sun for numerous vulnerable population groups (e.g. pregnant women, light-coloured skins etc., as described by the World Health Organization) [36]. Due to the lack of sources for SSA in the UV region, it is a common practice when estimating UV or forecasting health-related variables such as the UV index, to transfer SSA values from available visible wavelengths to UV wavelengths in radiative transfer calculations or just use climatological values [31].

This work aims to quantify the impact of spectral SSA (measurements and estimations) in the UV spectral region on UVA and UVB simulations from RTMs. Five years of measurements from CIMEL and UVFMR in Athens, Greece were used to retrieve SSA in the UV part of the solar spectrum, alongside with climatological means from satellite observations of the same period. Different SSAs from these methods were used as inputs in RTM and the results have been compared in order to obtain a robust estimation of the impact of SSA on UV irradiance. Also, actual irradiance measurements from a collocated Brewer spectroradiometer at 324 nm were used to validate the RTM results for different SSA inputs.

2. Data and methods

Aiming to quantify the effect of the absorbing/scattering nature of aerosols, the main physical variables used are SSA and absorption aerosol optical depth (AAOD). SSA at a wavelength λ is defined as the relative contribution of aerosol scattering extinction (b_{sca}) to total extinction ($b_{sca}+b_{abs}$), thus indirectly describing also the absorption contribution (b_{abs})

$$SSA=(b_{sca}(\lambda))/(b_{sca}(\lambda)+b_{abs}(\lambda)), (1)$$

Values of SSA range from 0 to 1 by definition; yet, in Earth's atmosphere, they are very rarely lower than 0.65 [7].

AAOD is calculated in respect to AOD and SSA as follows:

$$AAOD(\lambda)=AOD(\lambda)*(1-SSA(\lambda)), (2)$$

This variable is convenient for quantifying the final effect of the variations of aerosol absorption on radiative forcing, because it takes into account both the total extinction by aerosols and the scattering portion and, as such, cases of high AOD and low SSA, which lead to the largest reduction of irradiance, are more clearly identified.

The ground-based measurements used in this study were recorded during the period 2009-2014 in Athens, Greece. The site of the measurements was the roof of Biomedical Research Foundation of the Academy of Athens (37º 54'N, 23º 48'E, 130m above sea level), near the city centre, where the ground-based Atmospheric Remote Sensing Station (ARSS) was in continuous operation during this period [37]. Part of the ARSS infrastructure are a CIMEL sun-photometer and a UVMFR that were used in the present study. On the same roof, there was also a Brewer MKIV single monochromator installed.

2.1UVMFR

UVMFR is an instrument manufactured by Yankee Environmental Systems (http://www.yesinc.com), designed to measure Global and Diffuse Horizontal Irradiance at UV wavelengths. Incoming Irradiance is filtered and recorded at

channels centered around seven bandwidths (300, 305, 311, 317, 325, 332 and 368 nm) with Nominal Full Width Half Maximum at 2 nm. Each measurements cycle lasts 10 seconds and averaged 1 minute values are stored. In each cycle, two Diffuse Horizontal Irradiance (DHI) and one Global Horizontal Irradiance (GHI) measurements are performed, defined by the position of a moving shadowing disc. Thus, all data are recorded using the same sensor and the Direct Nominal Irradiance (DNI) is retrieved by subtracting DHI from GHI. Also, corrections for dark current and angular response are applied [23].

Kazadzis et al. [8] have developed a method for retrieving SSA at 332 and 368 nm using UVMFR measurements. This method is described in detail in the abovementioned work while in the present study a short outline is presented. Ratios of DHI/GHI are calculated for every measurement at 332 and 368 nm. Also, AOD is calculated at these wavelengths for each measurement. RTM calculations were performed using the Libradtran [38] code and lookup tables (LUT) were created linking DHI/GHI ratios and other variables such as Solar Zenith Angle (SZA) , AOD and SSA. Thus, a model was developed to calculate the SSA at each wavelength using these LUTs, as follows:

$$SSA(\lambda)=f(DHI(\lambda)/GHI(\lambda), SZA, AOD(\lambda)), \quad (3)$$

where λ indicates the wavelength. The method benefits from the technical fact that both DHI and GHI are measured by the same sensor, so there is no absolute calibration related uncertainty. Uncertainty analysis performed in Kazadzis et al. [8] revealed a final mean SSA error of the order of 5% for Athens' dataset, which might even exceed 15% in cases of very low aerosols (AOD <0.1) and very low SZA (<20º). At this study, we have used the same UVMFR dataset and model runs for the exact same period.

It should be noted that the determination of both AOD and SSA from the UVMFR instrument at wavelengths lower than 332nm is highly uncertain due to the total column ozone effect on solar irradiance attenuation [39]. The determination of the SSA using this method becomes even more difficult at such low wavelengths, as the uncertainty in the AOD retrieval introduces additional uncertainty to the SSA retrieval. For this purpose, AOD and SSA from UVMFR at 368nm for UVA and at 332nm for UVB related model runs have been used. Although 332 nm is in UVA region, it is used for this study's UVB RTM calculations as it is the closest wavelength with robust AOD retrieval. The uncertainty introduced by this choice could vary, according to Ångstrom Exponent in the UVB region, which could be up to 1.3% for AOD at 305 nm.

2.2 AERONET

CIMEL sun-photometers are the standard instruments of AERONET (Aerosol Robotic Network). Holben et al. [9] present a detailed description of the CIMEL instruments and AERONET protocols. These devices record DNI at eight

wavelengths and use the measurements at seven of the eight overall channels to retrieve AOD, while measurements of the eighth channel are used to retrieve the total column of water vapor. CIMEL sun-photometers also have a sky radiance measurement schedule at almucantar planes. These sky radiances are imported to a RTM model and inversion products are exported based on various hypotheses. These products include radiative properties such as SSA, phase function and asymmetry parameter. SSA is calculated at four wavelengths (440, 675, 870, 1020 nm). Level 2 (L2) data that are quality assured for SSA are produced only when AOD at 440 nm exceeds 0.4 and SZA exceeds 50º [40]. In this study, in order to enrich the dataset, we have also used Level 1.5 SSA data when L2 size distribution was available (as suggested by Kazadzis et al. [8]), since the limitation of L2 filtered out an important part of the retrievals for Athens dataset, where AOD>0.4 is not often.

2.3 Brewer spectrophotometer

Measurements of global and direct spectral UV irradiance have been routinely conducted at ARSS, since July 2003 on daily basis by a Brewer MKIV monochromator measuring solar radiation in the UV and the visible part of the solar spectrum. The instrument measures columnar amounts of ozone (Total Ozone Column – TOC), SO_2 and NO_2. It is also, measuring global (horizontal) irradiances in the UV-B part (290-315 nm) of the spectrum at 0.5 nm intervals. For total column ozone measurements, the instrument is designed to take direct sun measurements at five nominal wavelengths 306.3, 310.1, 313.5, 316.8 and 320.0 nm which are used with the standard algorithm to retrieve columnar ozone measurements from Brewer spectrophotometers [41]. Brewer ozone data for Athens have been analysed in recent studies [42,43]. In addition, the instrument was used to derive AOD in the visible part of the solar spectrum [44]. In this study, we analyse for the first time spectral UV irradiance measurements at 324 nm from the Athens Brewer instrument, for the period January 2009 to December 2014. The Brewer spectroradiometer is calibrated regularly by means of a standard radiometer of the same type. The last three calibrations were performed at the Academy of Athens in July 2007, October 2010 and October 2013 by the travelling standard Brewer #017 (International Ozone Services Inc., Mr. Ken Lamb and Dr. Volodya Savastiouk).

2.4 AEROCOM

The Max-Planck-Institute Aerosol Climatology version 1 (MAC-v1) provides optical properties of the total column of tropospheric aerosols, such as the AOD, the SSA and the asymmetry parameter [45]. The parameters are provided on monthly timescales for the entire globe, with spatial resolution of 1° × 1°. They have been derived by combining ground-based monthly statistics for aerosol optical properties from sun-photometer networks with the median of 15 AeroCom models [46]. Climatology was initially created for the mid-visible aerosol column optical properties, since reliable ground-based measurements exist mainly for the visible range of the solar spectrum, and was later extended to other wavelengths of the solar

and the far - infrared spectrum (ranging from 0.23 to 8 μm and 3.6 to 100 μm respectively) with the proper assumptions. In the UV region (UV-C, UV-B and UV-A) the optical properties are provided for 0.23, 0.3 and 0.4 μm. A linear interpolation of the desired parameters to the coordinates of ARSS was applied, since the coordinates of the ARSS do not coincide with any of the climatology grid points. The MAC-v1 climatology has been widely used in studies involving aerosols [31, 47, 48].

2.5 OMI

Aura satellite launched in 2004 by NASA carries the Ozone Monitoring Instrument (OMI). OMI scans the entire earth's surface in 15 orbits, with a ground spatial resolution of ~13X24km^2, measuring reflected radiation in 20 bandwidth channels in the spectral region of 270-500nm [27]. UV aerosol index, AOD and SSA are retrieved at 342.5 and 388nm using OMAERO algorithm, while there are also aerosol products from the OMAERUV algorithm which are a continuation of the Total Ozone Mapping Spectrometer time series [49]. The algorithm has been revised, by adding a more sophisticated carbonaceous aerosol model [6], and by including a spectral dependent imaginary index as a proxy for organics in the mixture [50]. This satellite product has major sources of uncertainty caused by cloud contamination, the height of aerosol layer and the hypothesis of surface albedo, especially in desert areas [28]. In the present study, we have used SSA and AOD from OMAERO, averaged at monthly level, using only 2009-2014 data, for the pixel including the location of the ground-based instruments. These data are available at https://disc.gsfc.nasa.gov/datasets/OMAERO_V003/summary.

2.6 Radiative Transfer Model

For RTM calculations the Libradtran code [38,51] was used. Multiple runs were performed in order to construct appropriate LUTs. Output spectra were set to 0.1 nm resolution for both GHI and DNI. Input values for AOD were 0-1.5 with a step of 0.1, for SZA 1-81º with a step of 2.5º, for SSA 0.60-0.96 with a step of 0.02 and for TOC 250-400DU with a step of 15 DU. As described in section 2.1, the output was used to calculate SSA from UVMFR measurements. Also, these output data were used to calculate Irradiance in the UV spectral region. UVA was calculated by integrating GHI values between 315-400 nm and between 305-315nm for UVB accordingly. Since the aim of the present work is to investigate the difference in irradiance caused by different estimation of SSA, other variables, such as Ångstrom Exponent, TOC and NO_2, and surface albedo, were used as constant inputs, using Athens climatology. Thus, the parametrization used is as follows:

$$UVA = f(AOD_{368}, SSA_i, SZA) \quad (4)$$

$$UVB = f(AOD_{332}, SSA_i, SZA) \quad (5)$$

Wherein, SZA is derived from astronomical calculations and SSA_i is used differently in each of the retrieved or the climatological (AEROCOM) datasets. For UVA and UVB, AOD retrieved with UVMFR at 368 nm and at 332 nm was used respectively. The uncertainty of this choice is discussed in section 2.1. TOC were set to climatological values and US Standard aerosol profiles were used [52] and maintained the same in all sets of runs to avoid any effect on the comparisons. NO_2 was also set to a constant mean climatological value. Keeping constant values for all inputs except aerosol parameters and sun elevation, provide the opportunity to study the SSA effects on UV solar irradiance, only. In order to validate the RTM outputs when comparing to Brewer measurements, RTM runs have been calculated using an Extraterrestrial Irradiance (at the top of the atmosphere) convoluted with the Brewer slit function, in order to have comparable results [53]. Modelled UVA and UVB values were calculated by integrating the RTM output irradiances at 315-400 nm and 290-315 nm accordingly. Comparison between RTM and Brewer UV irradiances at 324 nm was done using 324±1 nm integrals. The choice of this wavelength was to minimize the ozone effect on the absolute comparison differences [54].

3. Results and discussion

5 year average SSA recorded at 332 nm and 368 nm retrieved from UVMFR and at 440 nm from CIMEL are presented at figure 1, alongside with error bars at 1 standard deviation. Averages have been calculated separately for all data, for data with AOD higher than 0.2 and for data with Ångstrom Exponent lower than 0.7 which is linked to the presence of large and most frequently dust aerosols [8]. We can observe a systematic decrease of SSA values when moving from visible to lower wavelengths for the whole dataset. Using all AOD data we observe a drop of SSA from 440nm to 332nm of ~0.075, while for AOD>0.2 data the drop is smaller (~0.04). For dust aerosol cases SSAs are in general lower by ~0.05 for all wavelengths, showing a drop of ~0.07 from 440nm to 332nm. More details about this dependence can be found in [8].

Preprints (www.preprints.org) | NOT PEER-REVIEWED | Posted: 25 June 2018 doi:10.20944/preprints201806.0402.v1

Peer-reviewed version available at Atmosphere 2018, 9, 364; doi:10.3390/atmos9090364

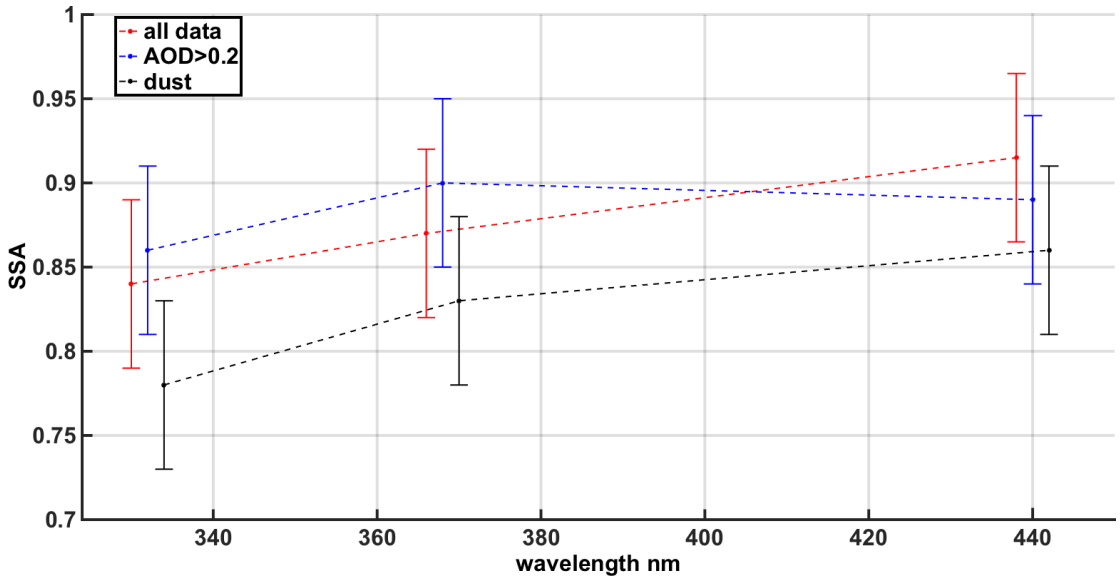

Figure 1. Mean SSA in UV and lower visible wavelengths, as measured in Athens for the period 2009-2014 (332 and 368nm measured by UVMFR and 440nm measured by CIMEL). Averages for all data, for AOD>0.2 and for dust cases (Ångstrom Exponent <0.7), are shown with different colors.

Based on the differences visualised in figure 1, we calculated the theoretical differences between UVB and UVA irradiances simulated by the RTM, with different SSA inputs. The example shown in figure 2 includes two cases: the first one using the CIMEL Athens mean SSA at 440nm (SSA_{440}) (0.91) and the second using the 368nm and 332nm SSA mean values from UVMFR (0.86 and 0.84 respectively). A graphical representation of the differences in each case is provided for all SZAs and AODs. The difference on the solar UV irradiance between the simulations for the two cases (using SSA_{440} or SSA from the UVMFR) is shown as a function of SZA and AOD. The differences are of the order of 10-13% and 13-18% per unit of AOD for UVA and UVB respectively. Although in Athens dataset, AOD of 1 is very rare, in such occasions UVB estimation could be different by 20%, which would introduce a very high error in UV index calculation and forecasts. In cases of very low AOD (<0.1) the differences are <2%, thus any differences on UVA and UVB estimations due to the spectral variability of SSA is less important. Highest relative differences are found at higher SZAs, which is linked to longer optical paths, and are expected to have a larger effect on aerosol extinction on solar irradiance.

Preprints (www.preprints.org) | NOT PEER-REVIEWED | Posted: 25 June 2018 doi:10.20944/preprints201806.0402.v1

Peer-reviewed version available at Atmosphere 2018, 9, 364; doi:10.3390/atmos9090364

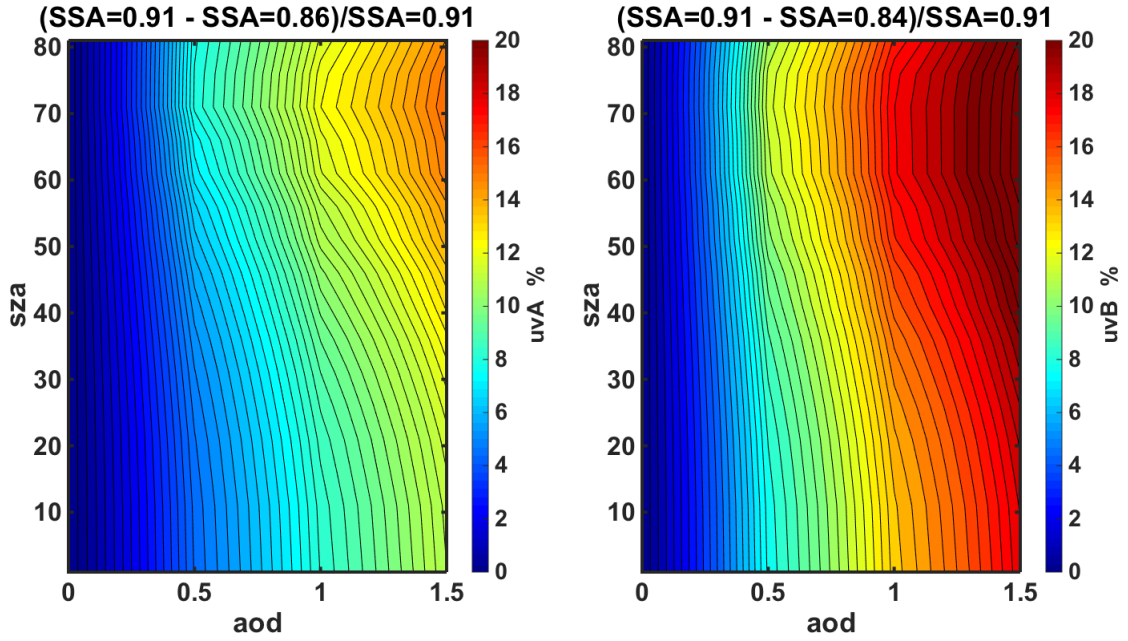

Figure 2. Relative differences of UVA (left) and UVB (right) irradiances for different SSAs as a function of SZA and AOD, calculated from RTM.

In order to perform the simulations using AOD and SSA from other available datasets, we have calculated the mean monthly values of SSA from OMAERO (388nm and 340nm), OMAERUV (388nm) and AEROCOM (300nm) for Athens, Greece and compared them to those from UVMFR (332 nm and 368 nm) and CIMEL (440 nm) (see figure 3a). In addition, mean monthly AODs for 332, 368 and 440nm were calculated from UVMFR and CIMEL measurements respectively and presented in figure 3 low. All average values in both figures were calculated using data from the period 2009-2014, which provides a short-term climatology for the Athens region. All SSA values retrieved from ground observations have lower values during the period from February to May, which in Kazadzis et al. [8] was attributed to frequent dust events and high brown carbon emissions in the urban area. Meanwhile, the highest monthly values are recorded during the summer months, peaking in August. OMAERUV at 338nm retrieves clearly higher values even from visible wavelengths (CIMEL 440nm) except from January and December, where the values from both instruments are similar. UVMFR retrievals have the lowest values all year round, with the exceptions of January and April when AEROCOM retrieves slightly lower ones and January when CIMEL is lower. AEROCOM monthly values, calculated at 300nm, deviate from those of other retrievals, and noticeably from those of UVMFR at 332nm. OMAERO practically provide the same values all year round except in November, but still the values are significantly higher than any other retrieval. AOD at all wavelengths peaks in July, showing higher values during the summer months. Lowest AOD is recorded in December and January. Mean AOD at 332nm is higher during the whole year, showing differences from AOD at 440nm ranging from 0.05 in December up to 0.13 in July.

Preprints (www.preprints.org) | NOT PEER-REVIEWED | Posted: 25 June 2018 doi:10.20944/preprints201806.0402.v1

Peer-reviewed version available at Atmosphere 2018, 9, 364; doi:10.3390/atmos9090364

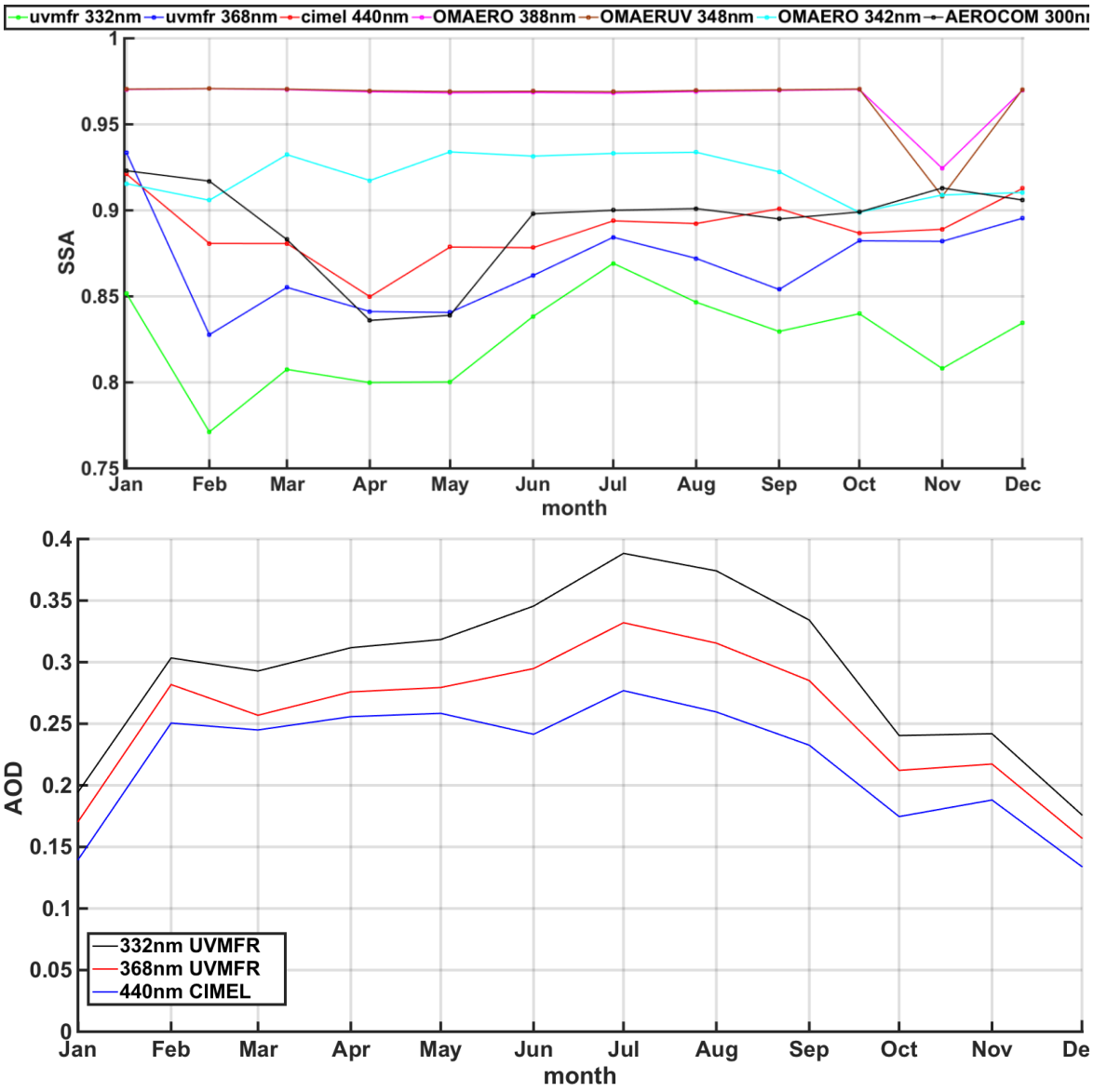

Figure 3. Top: Mean Monthly SSA values calculated by CIMEL and UVMFR time series and extracted from OMAERO, OMAERUV and Aerocom databases, for Athens during the 2009-2014 period. Bottom: mean monthly values of AOD calculated using CIMEL and UVMFR time series.

The differences between the simulations of UVB and UVA irradiance using UVMFR and CIMEL SSA inputs have been assessed. The inputs and model outputs presented here, can be seen in table 1. We have decided to keep the AOD inputs common (332 nm for UVB RTM integrals and 368 nm for UVA RTM ones) for all different data sources of SSAs in order to assess only the effect of differences in the SSA on simulated solar UV and not to mix (enhance) these differences by using (the slightly different but within the measurement uncertainty [8]), different AODs. Yet, this way guarantees a more robust comparison of the results, isolating SSA spectral related effects on UV irradiances.

Preprints (www.preprints.org) | NOT PEER-REVIEWED | Posted: 25 June 2018 doi:10.20944/preprints201806.0402.v1

Peer-reviewed version available at Atmosphere 2018, 9, 364; doi:10.3390/atmos9090364

Table 1: UVA and UVB Output Datasets of RTM runs, characterized by SSA and AOD used in each case. Result names are characterized by the SSA dataset used.

Name	AOD input (λ) (nm, instr.)	SSA input (λ) (nm, instr.)	Output (irradiance integral)
$UVMFR_{UVA}$	368,uvmfr	368,uvmfr	UVA
$UVMFR_{UVB}$	332,uvmfr	332,uvmfr	UVB
$CIMEL_{UVA}$	368,uvmfr	440,CIMEL	UVA
$CIMEL_{UVB}$	332,uvmfr	440,CIMEL	UVB
$OMAERO_{UVA}$	368,uvmfr	342, OMAERO	UVA
$AEROCOM_{UVB}$	332,uvmfr	300, Aerocom	UVB

Following this approach, mean UVA and UVB for each month was calculated for SZA=60º. This SZA selection was made to quantify the influence of different values of SSA excluding the seasonal variability of SZA and the SZA value was chosen as the one that can be found all year long. Relative differences of these results are presented in figure 4. These relative differences follow the combined seasonal variations of AOD and SSA, showing the lowest values in February reaching −9.1% for UVA and −12.3% for UVB. Barring UVA calculated with SSA_{CIMEL} and SSA_{UVMFR} in January, all other months reveal an underestimation of irradiance when using UVMFR inputs, which is explained by lower SSA values retrieved by the instrument. UVA calculated with SSA_{OMAERO} shows an average difference of 6.1% all year round as compared to the one calculated with SSA_{UVMFR}. UVA calculated with SSA_{CIMEL} has a yearly difference of 2.9% from that calculated with SSA_{UVMFR}. For UVB calculations, the relative differences are higher and are of the same order for both $SSA_{AEROCOM}$ and SSA_{CIMEL}, showing an average of −5.9% and −5.7% accordingly.

Preprints (www.preprints.org) | NOT PEER-REVIEWED | Posted: 25 June 2018 doi:10.20944/preprints201806.0402.v1

Peer-reviewed version available at Atmosphere 2018, 9, 364; doi:10.3390/atmos9090364

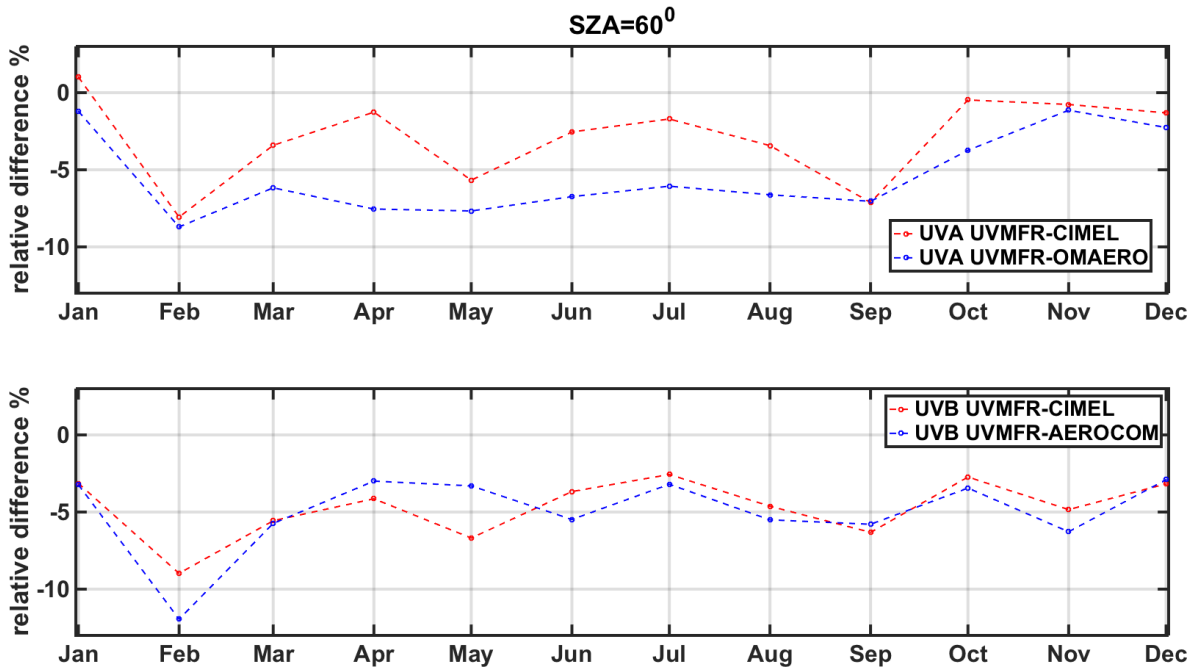

Figure 4: Mean Monthly Relative difference in UVA (upper plot) and UVB (lower plot), calculated with different SSA input and using time series of UVMFR SSA as reference.

Figure 5 shows the calculated differences for UVB and UVA outputs when using SSA_{CIMEL} and SSA_{UVMFR} as a function of AAOD. For these calculations, we have used all the 1480 synchronous values of both UVMFR and AERONET level 1.5 inversions products (following the criterion described in 2.2). AAOD was used for this comparison, as combined AOD and SSA changes in irradiance RTM outputs can be described by this parameter. This is because even if AODs did not differ in the compared model runs, irradiance differences are enhanced, due to higher AOD absolute values according to formula (2). In this particular figure, we can observe that UVB and UVA calculations, using SSA_{CIMEL} and SSA_{UVMFR} , decrease by ~12% per 0.05 of AAOD. When AAOD is higher than 0.04, an overestimation of outputs of SSA_{CIMEL} is the dominant case for both UVA and UVB, while the opposite appears in about 1% of the data. Although measurements of higher AAOD values would provide a more robust estimation of this behaviour, this estimation is produced using a 5 year long dataset and can be considered as representative for this urban area with moderate aerosol loads.

Preprints (www.preprints.org) | NOT PEER-REVIEWED | Posted: 25 June 2018 doi:10.20944/preprints201806.0402.v1

Peer-reviewed version available at Atmosphere 2018, 9, 364; doi:10.3390/atmos9090364

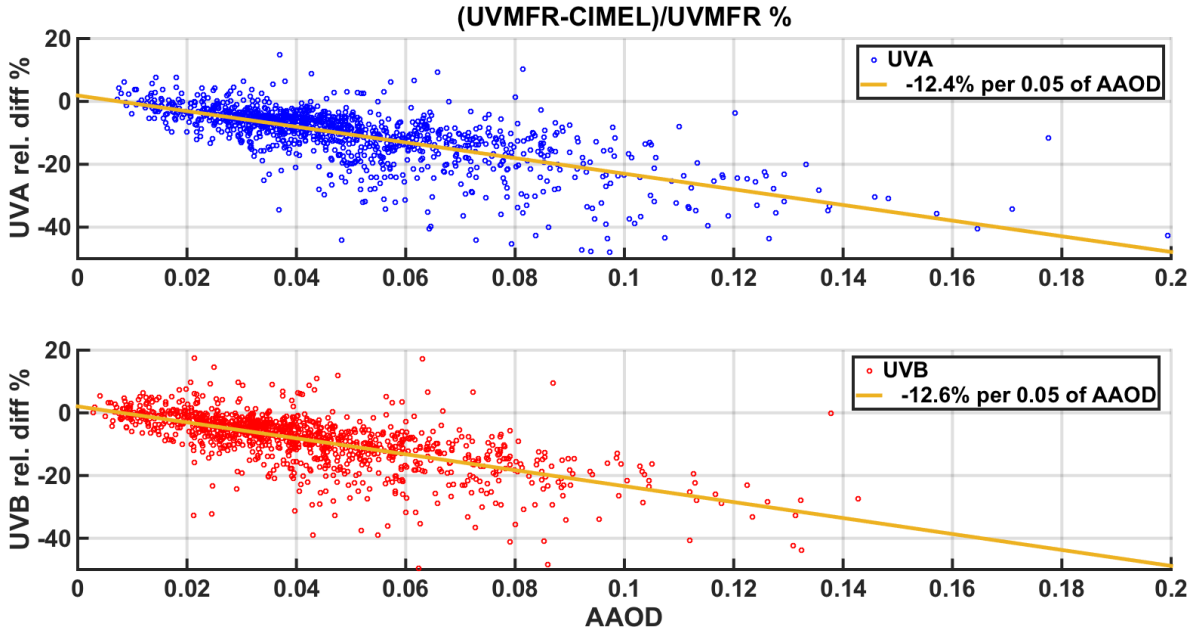

Figure 5. Relative difference in UVA (upper plot) and UVB (lower plot) with respect to AAOD, calculated with UVMFR and CIMEL SSA inputs as described in table 1

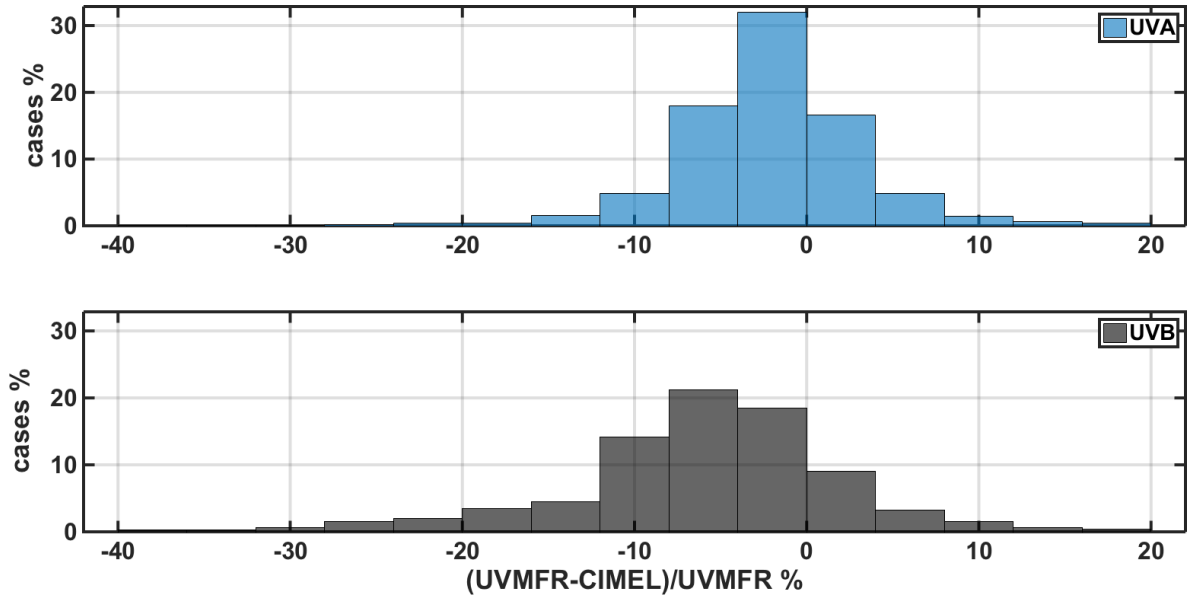

Figure 6. Relative Frequency Histograms of cases of UVA (upper plot) and UVB (lower plot) relative differences of GHI calculated using UVMFR and CIMEL SSA input as described in table 1, for all available synchronous data.

For the comparison of the full data set of UVMFR and CIMEL synchronous 1480 retrievals, the histograms presented in figure 6 were created. These histograms reveal a dominant overestimation of both UVA and UVB when calculated using SSA_{CIMEL}. The average relative difference for UVA is −4.7% and for UVB is −8.5%. For the 77.1% and 86.4% of the cases for UVA and UVB respectively, the irradiances simulated with input from SSA_{UVMFR} are lower than those simulated with SSA_{CIMEL}. The rest of the cases are linked with aerosol mixtures that have higher SSA in UV than in 440nm. These are usually expected to be fine mode absorbing aerosols and are attributed to urban pollution [8]. Also, there are very few cases (0.9% for UVA

Preprints (www.preprints.org) | NOT PEER-REVIEWED | Posted: 25 June 2018 doi:10.20944/preprints201806.0402.v1

Peer-reviewed version available at Atmosphere 2018, 9, 364; doi:10.3390/atmos9090364

and 1.4% for UVB) showing absolute differences higher than 25%. Kazadzis et al. [8] suggested that the majority of these cases are linked to Ångstrom Exponents lower than 0.7 and, thus, to severe dust events.

Aiming to verify the above results using actual solar irradiance measurements, we compare RTM simulated solar UV irradiances with synchronous cloud free Brewer UV measurements at 324 nm from the Brewer MKIV instrument that is located on the same roof as the UVMFR and CIMEL instruments. For this simulation, AOD_{UVMFR} and SSA_{UVMFR} at 332nm were used as input.

In order to validate the agreement between RTM and BREWER recorded Irradiance at 324nm, a statistical approach was selected. The statistical variables used are R^2 and root mean square error (RMSE) calculated as follows:

$$R^2 = 1 - \frac{\sum_i (y_i - f_i)^2}{\sum_i (y_i - <y>)^2} \quad (6)$$

$$RMSE = \sqrt{\frac{\sum_1^N (y_i - f_i)^2}{N-1}} \quad (7)$$

where y_i are the Brewer values, <y> is the average of those values, f_i are the calculated RTM and N is the number of measurements.

A comparison of 4297 synchronous cloud free (based on the cloud detection algorithm used for UVMFR [8]) Brewer measurements and UV_{324nm} model runs – with UVMFR input data - is shown in figure 7, demonstrating an R^2 of 0.96 and RMSE of 0.013W/m^2. The results show a good agreement with differences that can be mainly attributed to model inputs and measurement and absolute calibration uncertainties of the Brewer.

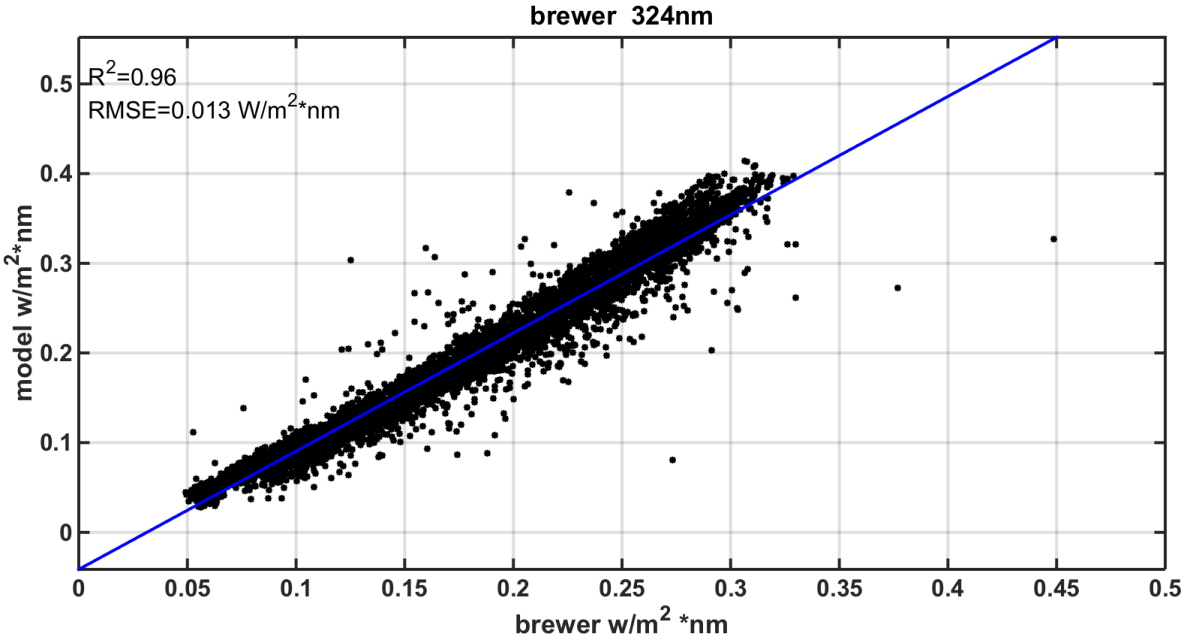

Figure 7: Cloudless synchronous retrievals of Global UV at 324nm, measured from Brewer and calculated from model using UVMFR SSA and AOD at 332nm inputs.

Finally, RTM runs were performed with CIMEL, AEROCOM and UVMFR 332nm SSA as well as UVMFR 332nm AOD and compared with Brewer recordings. At this scenario, AEROCOM values for the corresponding month, was used for all the synchronous UVMFR-BREWER data points. The distribution of differences of the three different scenarios is shown in Figure 8 and table 2. From these statistics, we conclude that irradiance calculated with SSA_{UVMFR} has the smallest absolute mean and median difference as compared to the ones calculated with SSA_{CIMEL} and $SSA_{AEROCOM}$. Results show a similar average difference with the ones shown in figure 6. Standard deviations of the differences are in the order of 6.5% to 7.5%. It is interesting that AEROCOM provides a slightly better agreement than AERONET, having smaller absolute mean and median differences. This is mainly because $SSA_{AEROCOM}$ is calculated at 300 nm. However, it is expected to have higher variation when using a constant climatological monthly value. It should be noted that the dominant case is the overestimation of simulated irradiance as compared to recorded values, which indicates that SSA at 324nm should be lower than any of these values. All three distributions have comparable range of values, with less than 10 cases of relative differences higher than 20%. Concluding the comparison, it appears that using SSA_{UVMFR} at 332 RTM UV_{324nm} calculation are the closest to Brewer measured results.

Table 2: Statistics of RTM calculated Irradiance at 324nm compared to Brewer recordings at 324 nm for all available data.

UV(Brewer-Model$_X$)/Brewer	Mean difference %	Standard Deviations %	Median %	5-95 percentile %
UVMFR	-0.85	6.78	-1.86	-9.72 – 11.24
CIMEL	-4.91	6.62	-5.58	-12.07 – 4.33
AEROCOM	-4.15	7.50	-5.34	-12.47 – 7.72

Preprints (www.preprints.org) | NOT PEER-REVIEWED | Posted: 25 June 2018 doi:10.20944/preprints201806.0402.v1

Peer-reviewed version available at Atmosphere 2018, 9, 364; doi:10.3390/atmos9090364

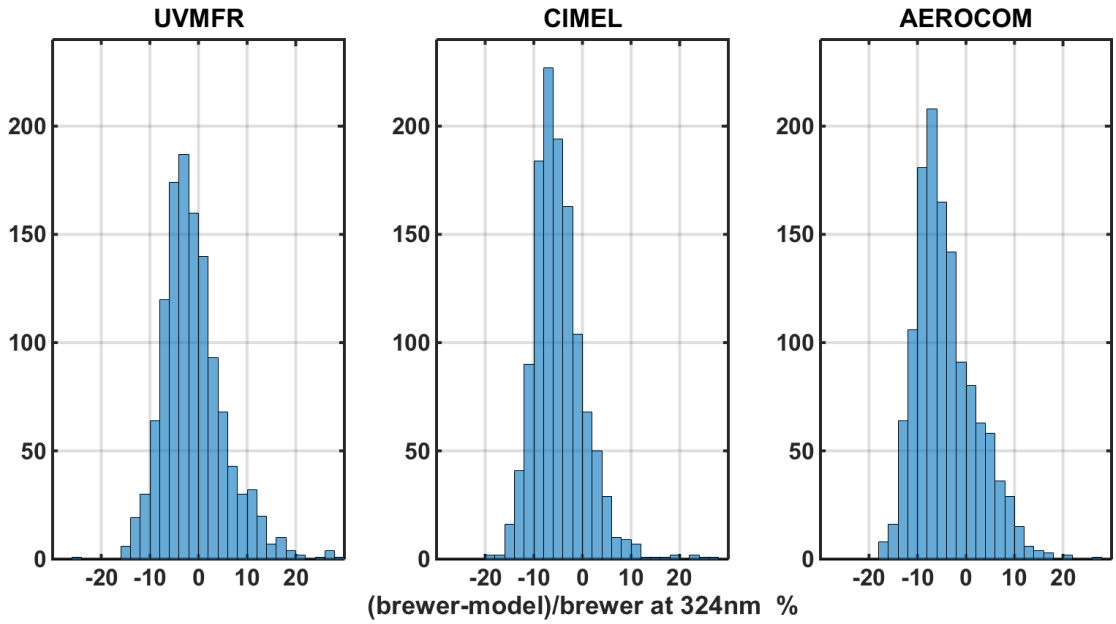

Figure 8. Number of cases of relative difference between Brewer recorded Irradiance at 324nm and estimated through RTM calculations using SSA_{UVMFR} at 332, SSA_{CIMEL} at 440nm and $SSA_{AEROCOM}$ at 300nm.

4. Conclusions

The effect of spectral SSA using different data sources for calculating incoming irradiance at UV wavelengths was studied. A 5 year long data set of SSA_{UVMFR} at 368 and 332 nm, AERONET retrievals at 440 nm, SSA_{OMAERO} at 342.5 nm and climatological values from AEROCOM were used as input to a RTM. Outputs were integrated to estimate UVA and UVB. Major findings are:

- SSA spectral decrease in the UV leads to a systematic overestimation of UV when SSA at visible is used, for the Athens area for the same AOD. The average difference for UVA is 4.7% and for UVB is 8.5% between estimations using SSA_{UVMFR} and SSA_{CIMEL} inputs.
- When climatological $SSA_{AEROCOM}$ values at 300nm were used to calculate UVB, average relative difference to the one calculated with SSA_{UVMFR} at 332 nm was found at 5.7%.
- The rate of underestimation of calculated UVA and UVB with SSA_{UVMFR} and SSA_{CIMEL}, for Athens, is -12% per 0.05 increase of AAOD. Mostly, for dust aerosol and local pollution related areas of the planet this overestimation could be highly important. In addition, as AAOD at lower (UVB) wavelengths is theoretically higher than the one at 332 nm the effect of using extrapolating SSA_{440} could have larger discrepancies in the UVB irradiance calculation than the results presented in this study.
- Comparison of UV Irradiance at 324nm from a Brewer, with RTM calculations using different SSA input was performed to validate the RTM results. It showed that using SSA_{UVMFR} at 332nm in the simulations provides closer to measured values with

a mean difference of 0.85%, compared to 4.91% when transferring SSA from the visible, and 4.11% when using climatological values.

Concluding it appears to be crucial for modelled UVA and UVB irradiance calculations a proper estimation of absorbing aerosol related columnar parameters such as SSA , especially when AOD is higher than 0.4. Although TOC is the major factor at UV wavelengths, especially in UVB region, SSA spectral dependence could lead to changes of more than 15% per unit of AOD. In the absence of SSA_{UV} measurements worldwide, currently used estimations for UV forecasts have a non-negligible uncertainty caused by the use of visible wavelength based SSA values.
All the above findings show the need of more detailed information on the aerosol absorbing properties in the UV range when UV related variables are estimated (UVA, UVB, UV Index, Vitamin D production), especially for high AOD areas.

Author Contributions "Conceptualization, Kazadzis S and Raptis PI.; Data Curation Raptis PI; Methodology, Raptis PI and Kazadzis S. and Fountoulakis I; Software, Raptis PI.; Validation, Raptis PI and Eleftheratos K.; Formal Analysis, Raptis PI and Kazadzis S.; Investigation, Raptis PI, Kazadzis S, Amiridis V and Elefhteratos K; Resources, Kazadzis, Amiridis V and Elefhteratos K.; Writing-Review Raptis PI Editing, Kazadzis S , Fountoulakis I. and Elefhteratos K.; Visualization, Raptis PI and Kazadzis S.; Supervision, Kazadzis S.; Project Administration, Kazadzis S and Raptis PI.",

Acknowledgements: This research was partly funded by the H2020 GEO-CRADLE project under grant agreement no. 690133. The research leading to these results was supported from the European Union's Horizon 2020 Research and Innovation Programme ACTRIS-2 (grant agreement no. 654109).

Conflicts of Interest: "The authors declare no conflict of interest."

References

1. Kaufman, Y.J., Tanré, D. and Boucher, O., A satellite view of aerosols in the climate system ,*Nature*, **2002**. *419(6903)*, p.215.
2. IPCC: Climate Change 2013: The Physical Science Basis. Contribution of Working Group I to the Fifth Assessment Report of the Intergovernmental Panel on Climate Change, edited by: Stocker, T. F., Qin, D., Plattner, G. K., Tignor, M., Allen, S. K., Boschung, J., Nauels, A., Xia, Y., Bex, V., and Midgley, P. M., Cambridge University Press, Cambridge, United Kingdom and New York, NY, USA, 1535 pp., doi:10.1017/CBO9781107415324, **2013**. Jacobson
3. Bergstrom, R.W., Pilewskie, P., Russell, P. B., Redemann, J., Bond, T. C., Quinn, P. K., and Sierau, B.: Spectral absorption proper- ties of atmospheric aerosols, *Atmos. Chem. Phys*., **2007**, *7*, 5937–5943, https://doi.org/10.5194/acp-7-5937-2007,
4. Mok, J., Krotkov, N.A., Arola, A., Torres, O., Jethva, H., Andrade, M., Labow, G., Eck, T.F., Li, Z., Dickerson, R.R. and Stenchikov, G.L.,. Impacts of brown carbon from biomass burning on surface UV and ozone photochemistry in the Amazon Basin. *Scientific reports*, **2016**, *6*,p.36940.
5. Martins, J. V., Artaxo, P., Kaufman, Y. J., Castanho, A. D., and Remer, L. A.: Spectral absorption properties of aerosol par- ticles from 350–2500 nm, *Geophys. Res. Lett.*, **2009**, *36*, L13810, https://doi.org/10.1029/2009GL037435, .
6. Jethva, H. and Torres, O.: Satellite-based evidence of wavelength-dependent aerosol absorption in biomass burning smoke inferred from Ozone Monitoring Instrument, *Atmos. Chem. Phys*., **2011**, *11(20)*, 10541–10551, doi:10.5194/acp-11-10541-2011.

7. Corr CA, Krotkov N, Madronich S, Slusser JR, Holben B, Gao W, Flynn J, Lefer B, Kreidenweis SM , Retrieval of aerosol single scattering albedo at ultraviolet wavelengths at the T1 site during MILAGRO. *Atmos Chem Phys*, **2009**, *9*, 5813–5827. doi:10.5194/acp-9-5813-2009
8. Kazadzis, S., Raptis, P., Kouremeti, N., Amiridis, V., Arola, A., Gerasopoulos, E. and Schuster, G.L., Aerosol absorption retrieval at ultraviolet wavelengths in a complex environment, *Atmospheric Measurement Techniques*, **2016**, *9(12)*, p.5997.
9. Holben, B.N., Eck, T.F., Slutsker, I., Tanre, D., Buis, J.P., Setzer, A., Vermote, E., Reagan, J.A., Kaufman, Y.J., Nakajima, T. and Lavenu, F., AERONET—A federated instrument network and data archive for aerosol characterization. *Remote sensing of environment*, **1998**, *66*(1), pp.1-16.
10. Kazadzis, S., Kouremeti, N., Diémoz, H., Gröbner, J., Forgan, B.W., Campanelli, M., Estellés, V., Lantz, K., Michalsky, J., Carlund, T. and Cuevas, E., Results from the Fourth WMO Filter Radiometer Comparison for aerosol optical depth measurements. *Atmospheric Chemistry and Physics*, **2018**, *18*(5), pp.3185-3201.
11. Remer, L.A., Kaufman, Y.J., Tanré, D., Mattoo, S., Chu, D.A., Martins, J.V., Li, R.R., Ichoku, C., Levy, R.C., Kleidman, R.G. and Eck, T.F., 2005. The MODIS aerosol algorithm, products, and validation. *Journal of the atmospheric sciences*,**2005**, *62*(4), pp.947-973.
12. Reid, J. S. and Hobbs, P. V.: Physical and optical properties of young smoke from individual biomass fires in Brazil, *J. Geophys. Res.-Atmos.*, **1998**, *103*, 32013–32030, 6448, 6457
13. Russell, P. B., Bergstrom, R.W., Shinozuka, Y., Clarke, A. D., De- Carlo, P. F., Jimenez, J. L., Livingston, J. M., Redemann, J., Dubovik, O., and Strawa, A.: Absorption Angstrom Exponent in AERONET and related data as an indicator of aerosol composition, *Atmos. Chem. Phys.*, **2010**, *10*, 1155–1169, doi:10.5194/acp-10-1155-2010.
14. Schwarz, J. P., Spackman, J. R., Gao, R. S., Watts, L. A., Stier, P., Schulz, M., Davis, S. M., Wofsy, S. C., and Fahey, D. W.: Global-scale black carbon profiles observed in the atmosphere and compared to. models, *Geophys. Res. Lett.*, **2010**, *37*, L18812, doi:10.1029/2010GL044372.
15. Skeie, R. B., Berntsen, T. K., Myhre, G., Tanaka, K., Kvalevåg, M. M., and Hoyle, C. R.: Anthropogenic radiative forcing time series from pre-industrial times until 2010, *Atmos. Chem. Phys.*, **2011**, *11*, 11827–11857, doi:10.5194/acp-11-11827-2011.
16. Andrews, E., Ogren, J. A., Kinne, S., and Samset, B.: Comparison of AOD, AAOD and column single scattering albedo from AERONET retrievals and in situ profiling measurements, *Atmos. Chem. Phys.*, **2017**, *17*, 6041-6072, https://doi.org/10.5194/acp-17-6041-2017.
17. Mok, J., Krotkov, N.A., Torres, O., Jethva, H., Li, Z., Kim, J., Koo, J.H., Go, S., Irie, H., Labow, G. and Eck, T.F., Comparisons of spectral aerosol single scattering albedo in Seoul, South Korea, *Atmospheric Measurement Techniques*, **2018**, *11(4)*, p.2295.
18. Holben, B. N., Tanré, D., Smirnov, A., Eck, T. F., Slutsker, I., Abuhassan, N., Newcomb, W. W., Schafer, J. S., Chatenet, B., Lavenu, F., Kaufman, Y. J., Castle, J. V., Setzer, A., Markham, B., Clark, D., Frouin, R., Halthore, R., Karneli, A., O'Neill, N. T., Pietras, C., Pinker, R. T., Voss, K., and Zibordi, G.: An emerging ground-based aerosol climatology: Aerosol optical depth from AERONET, *J. Geophys. Res.*, **2001**, *106*, 12067–12097, https://doi.org/10.1029/2001JD900014, https://doi.org/10.1029/2001JD900014.
19. Nakajima, T., Tonna, G., Rao, R., Boi, P., Kaufman,Y., and Holben, B.: Use of sky brightness measurements from ground for remote sensing of particulate polydispersions, *Appl. Optics*, **1996** , *35*, 2672– 2686, https://doi.org/10.1364/AO.35.002672.
20. Nakajima, T., Yoon, S.-C., Ramanathan, V., Shi, G.-Y., Takemura, T., Higurashi, A., Takamura, T., Aoki, K., Sohn, B.-J., Kim, S.-W., Tsuruta, H., Sugimoto, N., Shimizu, A., Tanimoto, H., Sawa, Y., Lin, N.-H., Lee, C.-T., Goto, D., and Schutgens, N.: Overview of the Atmospheric Brown Cloud East Asian Re- gional Experiment 2005 and a study of the aerosol direct radiative forcing in east Asia, *J. Geophys. Res.*, **2007** , *112*, D24S91, https://doi.org/10.1029/2007JD009009.
21. Bais AF, Kazantzidis A, Kazadzis S, Balis D, Zerefos CS, Meleti C, Effects of aerosol optical depth and single scattering albedo on surface UV irradiance, *Atmos Environ*, **2005**, *39*,1093–1102
22. Krotkov, N. A., Bhartia, P. K., Herman, J. R., Slusser, J. R., Labow, G., Scott, G. R., Janson, G. T., Eck, T. F., and Holben, B. N.: Aerosol ultraviolet absorption experiment (2002 to 2004), part 1: ultraviolet multifilter rotating shadowband radiometer calibration and intercomparison with CIMEL sunphotometers, *Opt. Eng.*, **2005** , *44*, 041004, https://doi.org/10.1117/1.1886818.
23. Krotkov, N. A., Bhartia, P. K., Herman, J. R., Slusser, J. R., Scott, G. R., Labow, G., Vasilkov, A. P., Eck, T. F., Dubovik, O., and Holben, B. N.: Aerosol ultraviolet absorption experiment (2002 to 2004), part 2:

absorption optical thickness, refrac- tive index, and single scattering albedo, *Opt. Eng.*, **2005** , *44*, 041005, https://doi.org/10.1117/1.1886819.

24. Kazadzis, S., Gröbner, J., Arola, A. and Amiridis, V. The effect of the global UV irradiance measurement accuracy on the single scattering albedo retrieval. *Atmospheric Measurement Techniques*, **2010**, *3*(4), p.1029.
25. Torres, O., A. Tanskanen, B. Veihelmann, C. Ahn, R. Braak, P. K. Bhartia, P. Veefkind, and P. Levelt , Aerosols and surface UV products from Ozone Monitoring Instrument observations: An overview, *J. Geophys. Res*., **2007** ,*112*, D24S47, doi:10.1029/2007JD008809.
26. Torres, O., C. Ahn, and Z. Chen, Improvements to the OMI near-UV aerosol algorithm using A-train CALIOP and AIRS observations, *Atmos. Meas. Tech*., **2013** , *6*, 3257–3270, doi:10.5194/amt-6-3257-2013
27. Ahn, C., O. Torres, and P. K. Bhartia , Comparison of Ozone Monitoring Instrument UVAerosol Products with Aqua/Moderate Resolution Imaging Spectroradiometer and Multiangle Imaging Spectroradiometer observations in 2006, *J. Geophys. Res*., **2008**, *113*, D16S27, doi:10.1029/ 2007JD008832
28. Jethva, H., O. Torres, and C. Ahn , Global assessment of OMI aerosol single-scattering albedo using ground-based AERONET inversion, *J. Geophys. Res. Atmos*., **2014**, *119*, 9020–9040, doi:10.1002/ 2014JD021672.
29. Asta, J., Pål, B., Arne, D., Stefan, A.-E., Jörg, R., Kristin, M., Michael, F. H., William, B. G., and Johan, M.: Solar radiation and human health, *Reports on Progress in Physics*, **2011**, *74*, 066701, 2011.
30. Lucas, R. M., Norval, M., Neale, R. E., Young, A. R., de Gruijl, F. R., Takizawa, Y., and van der Leun, J. C.: The consequences for human health of stratospheric ozone depletion in association with other environmental factors, *Photochemical & Photobiological Sciences*, **2015,** *14***,** 53-87, doi: 10.1039/c4pp90033b
31. Bais, A. F., McKenzie, R. L., Bernhard, G., Aucamp, P. J., Ilyas, M., Madronich, S., and Tourpali, K.: Ozone depletion and climate change: impacts on UV radiation, *Photochemical & Photobiological Sciences*, **2015**, *14*, 19-52.
32. Meleti, C., Bais, A. F., Kazadzis, S., Kouremeti, N., Garane, K., and Zerefos, C.: Factors affecting solar ultraviolet irradiance measured since 1990 at Thessaloniki, Greece, *International Journal of Remote Sensing*, **2009**, *30*, 4167-4179.
33. Fragkos, K., Bais, A. F., Fountoulakis, I., Balis, D., Tourpali, K., Meleti, C., and Zanis, P.: Extreme total column ozone events and effects on UV solar radiation at Thessaloniki, Greece, *Theor Appl Climatol*, **2016** , *126*, 505-517.
34. Fountoulakis, I., Bais, A. F., Fragkos, K., Meleti, C., Tourpali, K., and Zempila, M. M.: Short- and long-term variability of spectral solar UV irradiance at Thessaloniki, Greece: effects of changes in aerosols, total ozone and clouds, *Atmos. Chem. Phys*., **2016** , *16*, 2493-2505.
35. Castro T, Madronich S, Rivale S, Muhlia A, Mar B, The influence of aerosols on photochemical smog in Mexico City, *Atmos Environ*, **2001**, *35*,1765–1772. doi:10.1016/S1352- 2310(00)00449-0.
36. WHO, **2006**: Solar Ultraviolet Radiation: Global burden of desease from solar ultraviolet radiation. Environmental Burden of Disease Series, No. 13 (Authors: Lucas, R., McMichael, T., Smith, W., and Armstrong, B.; Editors: Pruss-Ustun, A., Zeeb, H., Mathers, C., and Repacholi, M.), World Health Organization, Public Health and the Environment, Geneva.
37. Amiridis, V., M. Kafatos, C. Perez, S. Kazadzis, E. Gerasopoulos, R. E. Mamouri, A.Papayannis, P. Kokkalis, E. Giannakaki, S. Basart, I. Daglis, and C. Zerefos, The Potential of the Synergistic Use of Passive and Active Remote Sensing Measurements for the Validation of a Regional Dust Model, *Annals Geophysics*, **2009**, *27*, 3155–3164. doi:10.5194/angeo-27-3155-2009
38. Mayer B, Kylling A, Technical note: the libRadtran software package for radiative transfer calculations – description and examples of use, *Atmos Chem Phys* , **2005**, *5*, 1855–1877
39. Carlund, T., Kouremeti, N., Kazadzis, S. and Gröbner, J., Aerosol optical depth determination in the UV using a four-channel precision filter radiometer. *Atmospheric Measurement Techniques*, **2017** ,*10*(3), p.905.
40. Dubovik O, King MD , A flexible inversion algorithm for retrieval of aerosol optical properties from Sun and sky radiance measurements, *J Geophys Res*, **2000**, *105 (D16*), 20,673–20,696. doi:10.1029/2000JD900282
41. Bais, A. F., Zerefos, C. S., Meleti, C., Ziomas, I. C. and Tourpali, K.: Spectral measurements of solar UV-B radiation and its relation to total ozone, SO_2, and clouds, *J. Geophys. Res*., **1993**, *98*, 5199-5204.
42. Kazantzidis, A., Bais, A. F., Zempila, M. M., Meleti, C., Eleftheratos, K., and Zerefos, C.: Evaluation of ozone column measurements over Greece with NILU–UV multi–channel radiometers, *International Journal of Remote Sensing*, **2009**,. *30*, Nos. 15-16, 4273–4281, doi: 10.1080/01431160902825073.

43. Raptis, P. I., Kazadzis, S., Eleftheratos, K., Kosmopoulos, P., Amiridis, V., Helmis, C., and Zerefos, C.: Total ozone column measurements using an ultraviolet multi-filter radiometer, *International Journal of Remote Sensing*, **2015**, *36(17),* pp.4469-4482.
44. Diémoz, H., Eleftheratos, K., Kazadzis, S., Amiridis, V., and Zerefos, C. S.: Retrieval of aerosol optical depth in the visible range with a Brewer spectrophotometer in Athens, A*tmos. Meas. Tech*., **2016**, *9*, 1871-1888, doi: 10.5194/amt-9-1871-2016.
45. Kinne, S., O'Donnel, D., Stier, P., Kloster, S., Zhang, K., Schmidt, H., Rast, S., Giorgetta, M., Eck, T.F. and Stevens, B., MAC-v1: A new global aerosol climatology for climate studies. *Journal of Advances in Modeling Earth Systems*, **2013**, *5*(4), pp.704-740.
46. Kinne, S., Schulz, M., Textor, C., Guibert, S., Balkanski, Y., Bauer, S. E., Berntsen, T., Berglen, T. F., Boucher, O., Chin, M., Collins, W., Dentener, F., Diehl, T., Easter, R., Feichter, J., Fillmore, D., Ghan, S., Ginoux, P., Gong, S., Grini, A., Hendricks, J., Herzog, M., Horowitz, L., Isaksen, I., Iversen, T., Kirkevåg, A., Kloster, S., Koch, D., Kristjansson, J. E., Krol, M., Lauer, A., Lamarque, J. F., Lesins, G., Liu, X., Lohmann, U., Montanaro, V., Myhre, G., Penner, J., Pitari, G., Reddy, S., Seland, O., Stier, P., Takemura, T., and Tie, X.: An AeroCom initial assessment – optical properties in aerosol component modules of global models, *Atmos. Chem. Phys.*, **2006**, *6*, 1815-1834, https://doi.org/10.5194/acp-6-1815-2006.
47. Ruiz-Arias, J.A., Dudhia, J. and Gueymard, C.A., A simple parameterization of the short-wave aerosol optical properties for surface direct and diffuse irradiances assessment in a numerical weather model. *Geoscientific Model Development*, **2014**, 7(3), pp.1159-1174.
48. Wilcox, L. J., Highwood, E. J., and Dunstone, N. J.: The influence of anthropogenic aerosol on multi-decadal variations of historical global climate, *Environmental Research Letters*, **2013**, *8*, 024033.
49. Torres, O., P. K. Bhartia, J. R. Herman, Z. Ahmad, and J. Gleason , Derivation of aerosol properties from satellite measurements of backscattered ultraviolet radiation: Theoretical basis, *J. Geophys. Res*., **1998** , *103(D14),* 17,099–17,110, doi:10.1029/98JD00900.
50. Kirchstetter, T. W., Novakov, T. & Hobbs, P. V., Evidence that the spectral dependence of light absorption by aerosols is affected by organic carbon,. *J. Geophys. Res.*, **2004**, *109*, D21208
51. Emde, C., Buras-Schnell, R., Kylling, A., Mayer, B., Gasteiger, J., Hamann, U., Kylling, J., Richter, B., Pause, C., Dowling, T. and Bugliaro, L., The libRadtran software package for radiative transfer calculations (Version 2.0), *Geoscientific model development discussions*, **2015**, *8*(12).
52. U.S. Standard Atmosphere, 1976, U.S. Government Printing Office, Washington, D.C..
53. Kazadzis, S., Bais, A., Kouremeti, N., Gerasopoulos, E., Garane, K., Blumthaler, M., Schallhart, B. and Cede, A., 2005. Direct spectral measurements with a Brewer spectroradiometer: absolute calibration and aerosol optical depth retrieval, *Applied optics*, **2005** , *44(9),* pp.1681-1690.
54. Fioletov, V.E., Kerr, J.B. and Wardle, D.I., the Relationship between Total Ozone and Spectral UV Irradiance from Brewer Observations and Its Use for Derivation of Total Ozone from UV Measurements. *Geophysical Research Letters*, **1997**, *24(23*), Pp.2997-3000.